

Enhanced Coherent Terahertz Emission from Critical Superconducting Fluctuations in $\text{YBa}_2\text{Cu}_3\text{O}_{6.6}$

D. Nicoletti^{1,*}, M. Rosenberg¹, M. Buzzi¹, M. Fechner¹, Y. Liu², S. Nakata², B. Keimer², R. A. Vitalone³, D. N. Basov³, P. E. Dolgirev⁴, E. Demler⁵, M. H. Michael¹ and A. Cavalleri^{1,6}

¹Max Planck Institute for the Structure and Dynamics of Matter, 22761 Hamburg, Germany

²Max Planck Institute for Solid State Research, 70569 Stuttgart, Germany

³Department of Physics, Columbia University, New York, New York 10027, USA

⁴Department of Physics, Harvard University, Cambridge, Massachusetts 02138, USA

⁵Institute for Theoretical Physics, ETH Zurich, 8093 Zurich, Switzerland

⁶Department of Physics, Clarendon Laboratory, University of Oxford, Oxford OX1 3PU, United Kingdom



(Received 3 April 2025; revised 4 July 2025; accepted 17 October 2025; published 24 November 2025)

Coherent terahertz (THz) emission is emerging as a powerful new tool to probe symmetry breakings in quantum materials. This method relies on second order optical nonlinearities and is complementary to second harmonic generation spectroscopy. Here, we report coherent THz emission from Josephson plasmons in underdoped $\text{YBa}_2\text{Cu}_3\text{O}_{6+x}$, and find that the amplitude of the emitted field increases dramatically close to the superconducting transition temperature, T_C . We show theoretically how emission is enhanced by critical superconducting fluctuations, a nonlinear analog of critical opalescence. This observation is expected to be of general importance for the study of many thermal and quantum phase transitions.

DOI: [10.1103/lbph-97sg](https://doi.org/10.1103/lbph-97sg)

Subject Areas: Superconductivity

I. INTRODUCTION

Coherent terahertz emission (CTE) spectroscopy is emerging as a powerful technique to probe subtle forms of symmetry breaking in complex solids [1,2]. Generally, CTE results either from optical rectification in noncentrosymmetric materials or from time dependent charge currents [3–7]. Several studies have demonstrated THz emission from complex materials, including colossal magnetoresistance manganites [6,8,9], magnetic compounds, and multiferroics [10–19].

In high- T_C superconductors, THz emission has been almost solely associated with time-dependent supercurrents generated by an external bias or magnetic field [7]. Among the various observations are near-single-cycle THz pulses in biased antennas fabricated from $\text{YBa}_2\text{Cu}_3\text{O}_{7-\delta}$ or $\text{Bi}_2\text{Sr}_2\text{CaCu}_2\text{O}_{8+\delta}$ films [4,20,21], multicycle narrowband emission governed by the Josephson effect in the presence of an applied out-of-plane magnetic field in $\text{Tl}_2\text{Ba}_2\text{CaCu}_2\text{O}_{8+\delta}$ films [22], and tunable, highly efficient narrowband emission

from MESA-type resonant structures made of Josephson junction stacks [23–25].

Recently, anomalous CTE was discovered in high- T_C cuprates of the $\text{La}_{2-x}\text{Ba}_x\text{CuO}_4$ (LBCO) family, in the absence of external magnetic fields and current biases [26]. This effect, which is forbidden by symmetry in this class of centrosymmetric materials, was detected only when superconductivity coexisted with *charge-stripe order* in the Cu-O planes [27], and when stripes [28–30] were either *incommensurate* with the lattice or *fluctuating*. These results were interpreted by reasoning that incommensurate (or fluctuating) charge density waves (CDW) [31,32] break inversion symmetry [32], and enable the emission by *surface Josephson plasmons* [33–35], finite momentum modes that are coupled into free space by the stripes.

In the present work, we show how charge-density-wave activated CTE exhibits striking anomalies when critical fluctuations of the order parameter set in close to T_C . This effect, which opens up a number of opportunities in the study of quantum phase transitions, is particularly clear in the case of $\text{YBa}_2\text{Cu}_3\text{O}_{6+x}$ (YBCO), in which the CDW survives across the superconducting phase transition, and could not be observed in LBCO, where T_C and T_{CDW} coincide.

$\text{YBa}_2\text{Cu}_3\text{O}_{6+x}$ has two Cu-O layers per unit cell and far higher superconducting critical temperatures than LBCO, up to ~ 90 K. As in LBCO and most cuprate families, YBCO is characterized by a dynamic charge ordering in the underdoped region of its phase diagram [36–39]. Fluctuating

*Contact author: daniele.nicoletti@mpsd.mpg.de

Published by the American Physical Society under the terms of the [Creative Commons Attribution 4.0 International license](https://creativecommons.org/licenses/by/4.0/). Further distribution of this work must maintain attribution to the author(s) and the published article's title, journal citation, and DOI. Open access publication funded by the Max Planck Society.

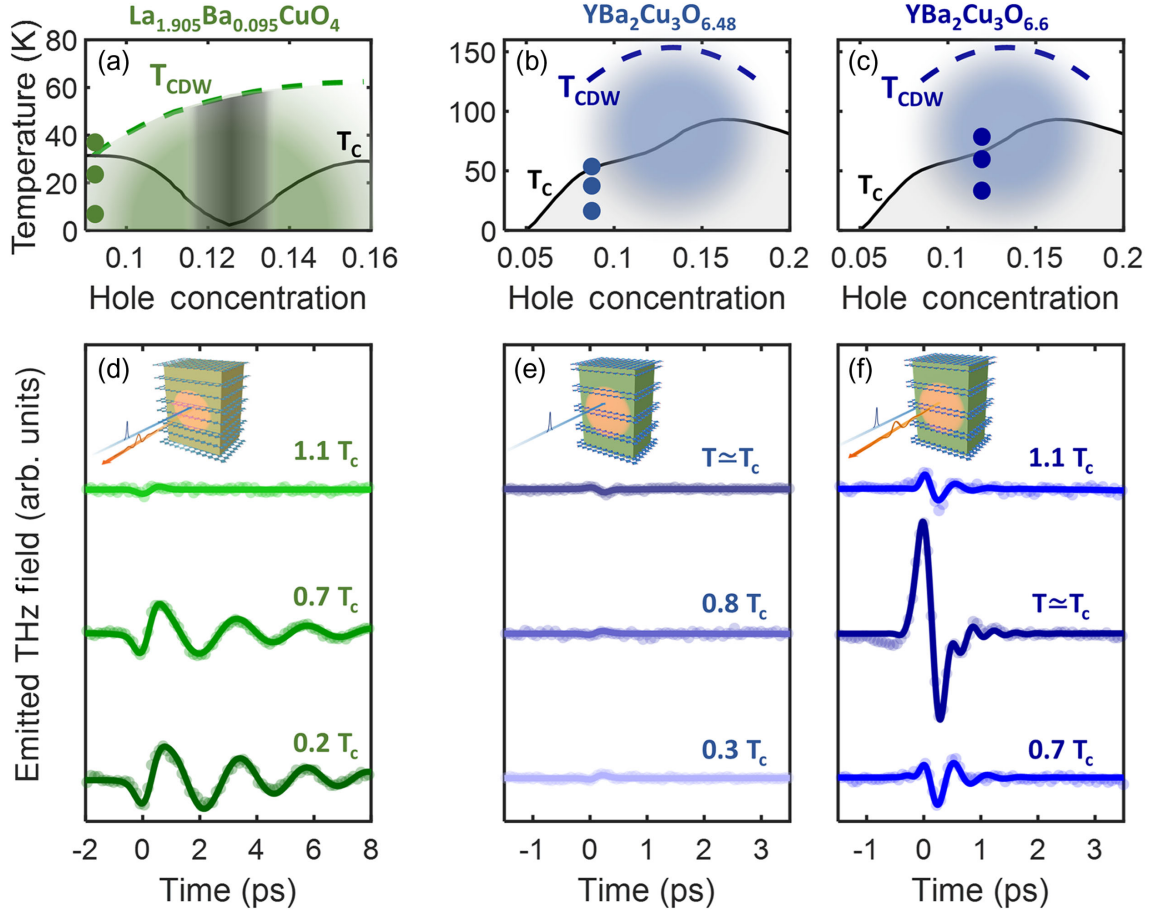


FIG. 1. (a)–(c) Temperature-doping phase diagrams of the compounds reported in the present study. T_{CDW} and T_{C} stand for the charge-density-wave ordering and the superconducting critical temperature, respectively [27,39]. (d)–(f) Time-dependent THz emission traces measured at the temperatures indicated by full circles in (a)–(c). Solid lines represent multicomponent fits [41] while experimental data are displayed as circles. The vertical scales in the three panels are mutually calibrated. Through a calibration with a ZnTe crystal mounted on the same sample holder, we estimate the peak THz fields in (d) and (f) to be no larger than ~ 10 V/cm. Data in (d) have been taken with a pump fluence of ~ 2.5 mJ/cm² [26], while those in (e)–(f) with ~ 5 mJ/cm². Insets: Experimental geometry. Near-infrared (NIR) pump pulses, with typical duration of ~ 100 fs, are shone at normal incidence onto an *ac*-oriented sample surface, with polarization parallel to the *c* axis (i.e., perpendicular to the Cu-O planes). As a result of photoexcitation, *c*-polarized THz radiation is emitted.

CDWs are found in compounds near $\text{YBa}_2\text{Cu}_3\text{O}_{6.6}$ (YBCO 6.6), corresponding to a hole concentration in the Cu-O planes close to 12.5%, vanishing rapidly for doping levels away from this value [39]. In YBCO 6.6 this charge-density-wave phase appears for temperatures as high as $T_{\text{CDW}} \simeq 150$ K, more than a factor of 2 higher than the superconducting T_{C} [see phase diagram in Figs. 1(b) and 1(c)], displaying a maximum in intensity exactly at T_{C} [39]. For lower temperatures, deep in the superconducting phase, the CDW gradually decreases and can be revived by the application of external magnetic fields, providing confirmation that it competes with superconductivity [40].

In contrast to LBCO, the CDW in YBCO is always fluctuating, as well as incommensurate with the crystal lattice (in-plane wave vector $q \simeq 0.33$). Moreover, the values of the CDW correlation length in YBCO, $\xi_{ab} \sim 50$ Å [39,40], are

similar to those found in LBCO 9.5% [27], the compound for which optimal conditions for THz emission were found.

For these reasons, we investigated the THz emission properties of $\text{YBa}_2\text{Cu}_3\text{O}_{6.6}$ ($T_{\text{C}} = 63$ K). These were compared with the response of $\text{YBa}_2\text{Cu}_3\text{O}_{6.48}$ (YBCO 6.48), with hole concentration $\sim 9\%$ and $T_{\text{C}} = 51$ K, a compound for which only a very weak CDW below $T_{\text{CDW}} \simeq 100$ K was reported [39].

II. EXPERIMENTAL RESULTS

The experimental geometry is shown schematically in the insets of Figs. 1(e) and 1(f). We used the output of an amplified Ti:sapphire femtosecond laser as pump pulses, with a duration of 100 fs and photon energy of 1.55 eV (800 nm wavelength). These were focused at normal

incidence onto an *ac*-cut sample surface, with polarization oriented along the out-of-plane (*c*) direction. The emitted THz pulses (also *c* polarized) were collimated with a parabolic mirror and refocused on a 1-mm-thick ZnTe crystal to perform electro-optic sampling, directly yielding THz electric field traces in time domain.

In Figs. 1(e) and 1(f) we report selected time traces of the emitted THz field, measured in both YBCO samples investigated in this study (see Supplemental Material [41] for extended datasets and Ref. [60] for source data). The temperatures at which these data were taken are displayed as full circles in the phase diagrams in Figs. 1(b) and 1(c). For completeness, we also show in Fig. 1(d) the emission traces taken in LBCO 9.5% and already reported in Ref. [26], with the corresponding phase diagram in Fig. 1(a). The vertical scales in Fig. 1(d)–1(f) have been kept the same, allowing a quantitative comparison between the emission amplitudes in different compounds.

As expected, we observed effectively no response in YBCO 6.48, a compound that shows a weak CDW phase [39] and for which we measured only a temperature-independent single cycle emission just above the noise level [Fig. 1(e)]. This result is very similar to what was reported for optimally-doped $\text{La}_{1.885}\text{Sr}_{0.16}\text{CuO}_4$ (no stripe order) and for $\text{La}_{1.885}\text{Ba}_{0.115}\text{CuO}_4$ (quasistatic stripes) in Ref. [26]. This weak single cycle emission, not relevant for the discussion in this paper, is tentatively attributed to the Dember field generated at the sample surface by photo-carrier electron-hole separation [61].

In contrast, at the doping levels corresponding to the most robust CDW [YBCO 6.6, see Fig. 1(f)], we found a significantly stronger response. Here, at the lowest temperature ($T \ll T_C$), the emitted field is already a factor ~ 5 larger than in YBCO 6.48. Unlike in LBCO 9.5%, in which the signal decreased for temperatures approaching T_C from below, following the amplitude of the stripes in that compound, in YBCO 6.6 the response grows dramatically with increasing temperature, reaching its maximum near T_C , and then reducing abruptly for $T > T_C$. The time traces are also qualitatively different from the coherent multicycle emission observed in LBCO 9.5% [Fig. 1(d)], showing instead a couple of cycles at most in YBCO 6.6 [Fig. 1(f)].

For a more detailed comparison between the emission properties of these two cuprates, we report in Fig. 2 Fourier transforms of the time traces of Figs. 1(d) and 1(f) [41]. Beyond the systematically narrower bandwidth found in LBCO 9.5% [41], the temperature dependencies are very different. On the one hand, in LBCO 9.5% the emission frequency progressively redshifts and its amplitude decreases with increasing temperature, disappearing across the transition. By contrast, in YBCO 6.6 we found (i) a gradual growth of the overall emission amplitude as temperature was increased, with a peak near T_C and (ii) a progressive redshift of the peak frequency, similar to that of LBCO 9.5%, with the appearance of a second frequency

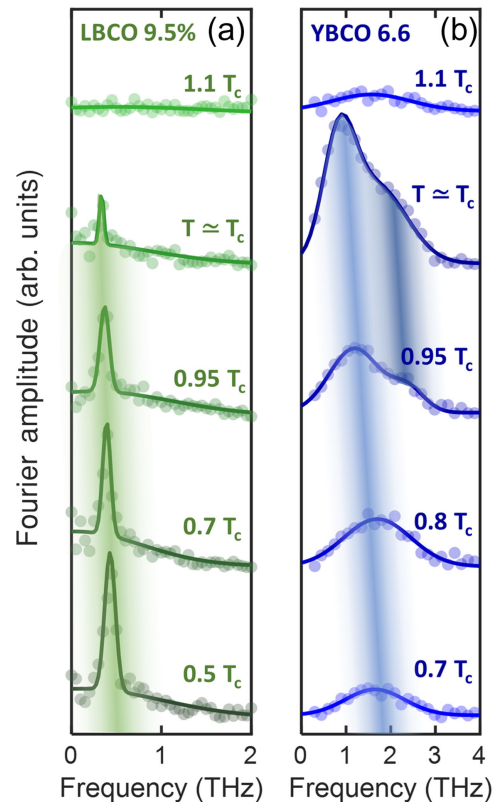


FIG. 2. Fourier transforms (circles) of the time-domain traces of Fig. 1, shown for both compounds for which we detected a sizeable THz emission, namely, $\text{La}_{1.905}\text{Ba}_{0.095}\text{CuO}_4$ (a) and $\text{YBa}_2\text{Cu}_3\text{O}_{6.6}$ (b). Solid lines are multi-Gaussian fits while full circles indicate the experimental data. Spectra are reported at selected temperatures above and below the superconducting T_C ($T_C = 33$ K for $\text{La}_{1.905}\text{Ba}_{0.095}\text{CuO}_4$ and $T_C = 63$ K for $\text{YBa}_2\text{Cu}_3\text{O}_{6.6}$). Data in (a) were taken with a pump fluence of ~ 2.5 mJ/cm² [26], while those in (b) with ~ 5 mJ/cm². The shadings track the temperature dependence of the peak emission frequency. Only for $\text{YBa}_2\text{Cu}_3\text{O}_{6.6}$ a second contribution at twice the fundamental frequency appears close to T_C .

component at twice the main emission frequency. Note that the Gaussian fits shown in Fig. 2(b) for data at $T = 0.95T_C$ and $T \approx T_C$ were performed by constraining the peak frequencies to be ω and 2ω .

In Fig. 3 we report a detailed temperature dependence of the peak emission frequencies for different excitation fluences. As in Ref. [26], we show a comparison with the Josephson plasma resonance measured at equilibrium with time-resolved THz spectroscopy in the same samples. Its exact frequency was determined by fitting the experimental reflectivity with a Josephson plasma model [26,41].

In both LBCO 9.5% and YBCO 6.6 the main emission frequency traces the temperature dependence of the Josephson plasma resonance, approaching it more and more closely for progressively lower fluences but always remaining at values slightly lower than ω_{JPR} by about 10%. This result confirms that in YBCO 6.6 the CTE mechanism

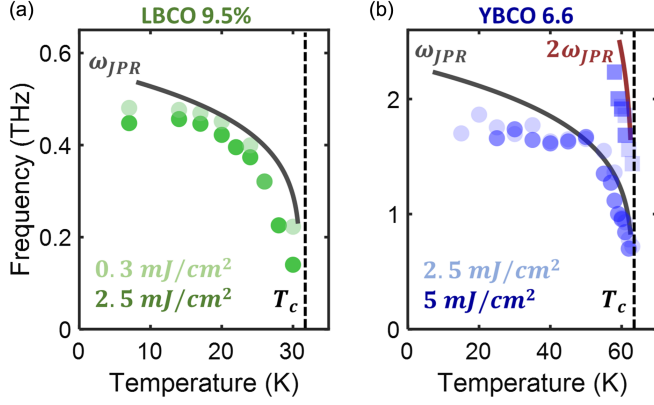


FIG. 3. Comparison between equilibrium Josephson plasma resonance (full black lines) and emission peak frequencies (circles) measured for different excitation fluences (see legend) in $\text{La}_{1.905}\text{Ba}_{0.095}\text{CuO}_4$ [26] and $\text{YBa}_2\text{Cu}_3\text{O}_{6.6}$. $\omega_{\text{JPR}}(T)$ was determined by shining a weak, c -polarized broadband THz pulse at normal incidence onto the sample surface and detecting the electric field profile of the same THz pulse after reflection. The data were then fitted with a Josephson plasma model [41]. In panel (b) we also compare $2\omega_{\text{JPR}}(T)$ (red line) with the second harmonic emission peak frequencies (blue squares), detected in $\text{YBa}_2\text{Cu}_3\text{O}_{6.6}$ at $T \lesssim T_c$.

must involve the optical excitation of Josephson plasmons, as similarly discussed for LBCO [26]. Moreover, the evidence of a systematic redshift of ω_{CTE} with respect to ω_{JPR} suggests that THz emission in both materials presumably originates from surface modes, whose dispersion curve lies entirely below the bulk Josephson plasma resonance (see Ref. [26] for further details on the proposed mechanism).

Even harmonics in the emission spectrum of YBCO 6.6 could originate from a large-amplitude excitation of anharmonic plasmons. This effect should be prohibited in a centrosymmetric layered structure, but could potentially be activated in the presence of a charge order-induced inversion symmetry breaking [26]. However, this mechanism driven by plasmon anharmonicities appears unlikely when looking at the amplitude scaling of the CTE. In the Supplemental Material [41] we plot the amplitude of the $2\omega_{\text{JPR}}$ peak against that of the peak at ω_{JPR} for various data sets taken at different temperatures and pump fluences. This shows a linear dependence and does not connect to a nonlinear plasmon emission, for which one would expect quadratic scaling [42].

III. MODEL FOR COHERENT TERAHERTZ EMISSION

We argue here that the anomalous linear scaling of second harmonic emission is a reporter of superconducting fluctuations. To substantiate this argument, we introduce a model that describes CTE from Josephson plasmons in cuprates with coexisting superconductivity and CDW. First,

we consider the time derivative of the Josephson current, $E_{\text{CTE}}(t) \propto [\partial/(\partial t)]j_{\text{JPR}}(t)$, as the source of CTE. According to the first Josephson equation, $j_{\text{JPR}}(t) = \omega_{\text{JPR}}^2 \sin \theta(t)$, which in the limit of small Josephson phase distortions is expressed as $j_{\text{JPR}}(t) \simeq \omega_{\text{JPR}}^2 \theta(t)$. Thus, the CTE amplitude scales linearly with the Josephson phase velocity, $\dot{\theta}(t)$, as $E_{\text{CTE}} \propto [\partial/(\partial t)]j_{\text{JPR}}(t) \simeq \omega_{\text{JPR}}^2 \dot{\theta}(t)$. Through the second Josephson equation, $\dot{\theta}(t) = \{[2eV_J(t)]/\hbar\}$, where $V_J(t)$ is the voltage drop across the junction, we obtain a direct proportionality between the emitted THz field, $E_{\text{CTE}}(t)$, and the electric field inside the Josephson junction, $E_J(t) = \{[V_J(t)]/d\}$ (here d is the junction size).

Based on our previous work [26,31,32], and having simplified in part the model by leaving out the full analysis of surface modes, we assume that the inherent symmetry breaking by incommensurate CDWs in LBCO 9.5% and YBCO 6.6 enables a Raman excitation process of Josephson plasmons. In this process, the rectified force of two optical photons from the drive induces coherent Josephson plasma oscillations with a strength that is directly proportional to the CDW intensity. Following the derivation reported in the Supplemental Material [41], the frequency-dependent CTE amplitude generated through this mechanism can be expressed as

$$|E_{\text{CTE}}^{\text{JPR}}(\omega, T)| = \left| \frac{I_{\text{CDW}}(T)\omega^2(\omega^2 + i\gamma_{\text{JPR}}\omega)}{-(\omega^2 + i\gamma_{\text{JPR}}\omega - \omega_{\text{JPR}}^2(T))^2} \right| E_{\text{opt}} E_{\text{opt}}, \quad (1)$$

where $I_{\text{CDW}}(T)$ is the temperature dependent CDW intensity [27,39], γ_{JPR} is a JPR damping coefficient, and E_{opt} denotes the field strength of the optical drive.

Notably, this CTE process is always enabled as long as the incommensurate CDW order is present, a condition that is met throughout the superconducting phase for both LBCO and YBCO compounds studied here. However, while YBCO 6.6 (for which $T_{\text{CDW}} \gg T_c$) exhibits a robust CDW phase across the superconducting transition [39], $I_{\text{CDW}}(T)$ becomes vanishingly small in LBCO 9.5% for $T \lesssim T_c = T_{\text{CDW}}$ [27], thus leading to the strong CTE suppression near T_c observed for this compound.

We next consider an additional contribution to CTE that originates from *second-order* Raman processes involving the excitation of *pairs* of Josephson plasmons, i.e., Josephson *biplasmons*, which appear as coherent Josephson plasma oscillations at $\omega = 2\omega_{\text{JPR}}$ [31,43,44,62,63], in a way similar in many aspects to biphonon excitations [64]. The strength of this new term depends critically on the amplitude of superconducting fluctuations and is therefore strongly enhanced close to T_c . In addition, its amplitude scales quadratically with the drive electric field, i.e., linearly with pump fluence, as observed for the $2\omega_{\text{JPR}}$ peak in our experiment on YBCO 6.6 [41].

In the Supplemental Material [41], we report an explicit derivation for this second CTE channel, according to which the emitted THz field amplitude is expressed as

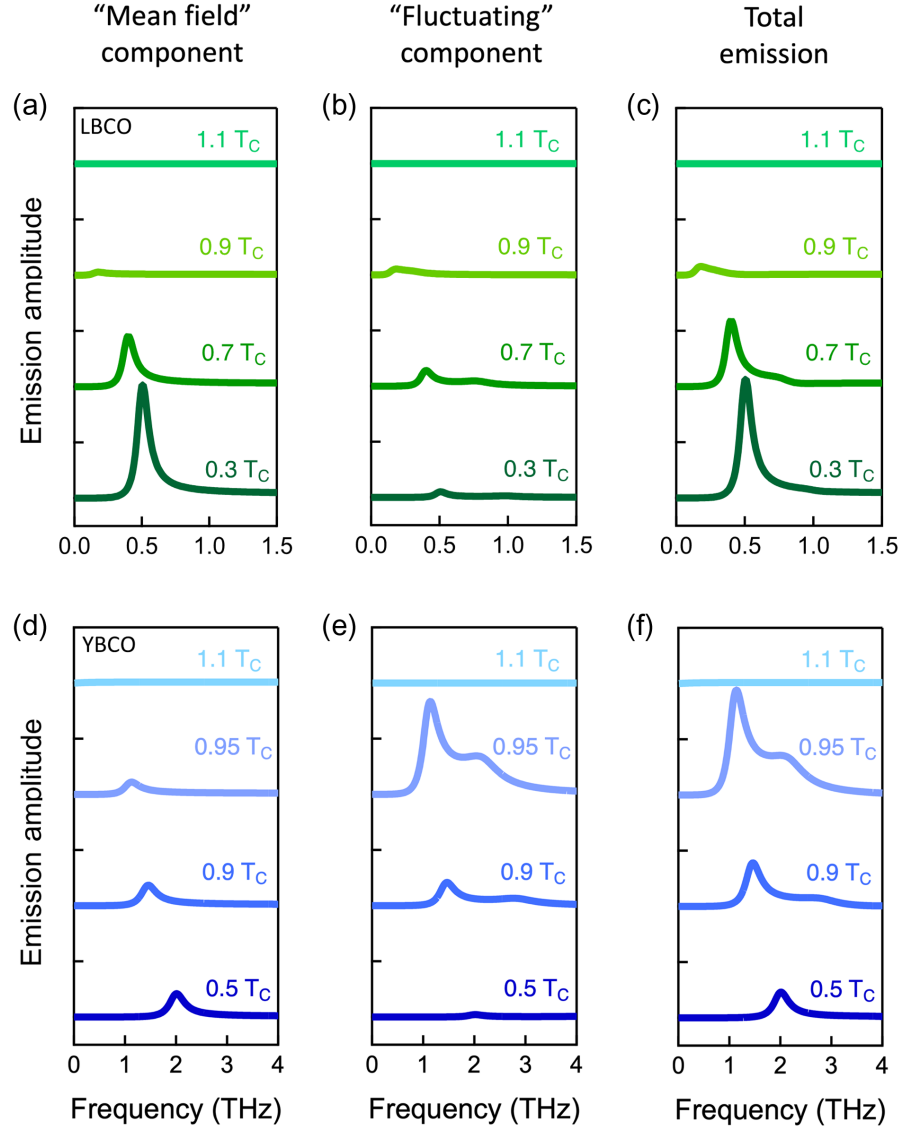


FIG. 4. THz emission spectra from LBCO 9.5% (a)–(c) and YBCO 6.6 (d)–(f) calculated with the model described in the main text at selected temperatures below and above the superconducting T_C . The different panels show the mean field (single-plasmon) contribution to the emitted field (a),(d), the bi-plasmon term related to superconducting fluctuations (b),(e), and the sum of the two, which gives rise to the total emission (c),(f).

$$|E_{\text{CTE}}^{\text{fluct}}(\omega, T)| = \left| A \frac{N_{\text{fluct}}(T) \omega_{\text{JPR}}^2(T)}{\omega^2 + 2i\gamma_{\text{JPR}}\omega - 4\omega_{\text{JPR}}^2(T)} \frac{I_{\text{CDW}}(T) \omega^2 (\omega^2 + i\gamma_{\text{JPR}}\omega)}{(\omega^2 + i\gamma_{\text{JPR}}\omega - \omega_{\text{JPR}}^2(T))^2} \right| E_{\text{opt}} E_{\text{opt}}, \quad (2)$$

where $N_{\text{fluct}}(T)$ denotes the temperature dependent amplitude of the superconducting fluctuations and A is a scaling factor. Note that in this analysis we have ignored the bilayer structure of YBCO [45–53] and approximated the Josephson dynamics as that of a single layered cuprate, like LBCO (see Supplemental Material [41] for validation of this approach).

In Fig. 4 we show calculated emission spectra for both compounds at selected temperatures, highlighting separately

the different components $|E_{\text{CTE}}^{\text{JPR}}(\omega, T)|$ (a),(d) and $|E_{\text{CTE}}^{\text{fluct}}(\omega, T)|$ (b),(e), that contribute to the overall radiated spectrum, $|E_{\text{CTE}}^{\text{tot}}(\omega, T)| = |E_{\text{CTE}}^{\text{JPR}}(\omega, T) + E_{\text{CTE}}^{\text{fluct}}(\omega, T)|$ (c), (f). For $T \ll T_C$ in both LBCO 9.5% and YBCO 6.6 the calculated emission is dominated by the mean field (single-plasmon) term, since $N_{\text{fluct}}(T)$ is vanishingly small. Close to T_C instead, the YBCO 6.6 spectrum is almost entirely attributable to the fluctuating (bi-plasmon) component and shows a prominent peak at $2\omega_{\text{JPR}}$ accompanied by a

subharmonic contribution at ω_{JPR} . In LBCO 9.5% on the other hand, superconducting fluctuations, although present at $T \lesssim T_C$, are silent, because $I_{\text{CDW}}(T)$ vanishes at T_C [27], causing the material to lack the prerequisite to radiate.

IV. COMPARISON WITH THE EXPERIMENTAL DATA AND DISCUSSION

In Fig. 5 we directly compare these predictions to experimental data. We extracted experimental values of $I_{\text{CDW}}(T)$ for both compounds from literature [27,39], and estimated $\omega_{\text{JPR}}(T)$ and $\gamma_{\text{JPR}}(T)$ from our THz spectroscopy measurements at equilibrium [41]. Using $N_{\text{fluct}}(T)$ and A as the only fit parameters, which we tuned to the response of YBCO and then kept fixed for LBCO, our model was able to consistently and quantitatively reproduce both the enhancement of peak emission and the appearance of a $2\omega_{\text{JPR}}$ contribution near T_C in YBCO 6.6, as well as the absence of these features in LBCO 9.5%. Our experiment reveals important new aspects of CTE from cuprates with coexisting superconductivity and charge-density-wave ordering. First, we see confirmation that the presence of fluctuating and/or incommensurate charge order is a fundamental ingredient to observe this phenomenon by providing the necessary inversion symmetry breaking. The

new data on YBCO 6.6, showing a systematic redshift of the emission peak frequency with respect to the Josephson plasma resonance at equilibrium, are compatible with the idea introduced for LBCO 9.5% in Ref. [26] that the emission likely occurs via the excitation of surface Josephson plasmons rather than bulk plasma polaritons. The new observation here concerns the anomalous enhancement of CTE near the superconducting transition as well as the appearance of a large second harmonic peak. This $2\omega_{\text{JPR}}$ contribution exhibits an anomalous linear scaling with pump fluence, which is consistent with the excitation of pairs of Josephson plasmons, as reproduced in detail by our model.

We have shown here that CTE probes quantum fluctuations of the superconducting condensate at $T \lesssim T_C$, where the impulsive Raman mechanism that triggers emission is boosted by these fluctuations. Qualitatively, the observations reported here are a nonlinear analog of critical opalescence, in which linear light scattering is enhanced by critical fluctuations. Given the indications that coherent THz emission in the superconducting state may be mediated by the excitation of surface rather than bulk Josephson plasmons, we envisage complementing far-field spectroscopy with other techniques sensitive to emission in the near field, such as scanning near-field optical microscopy in the terahertz range (THz-SNOM) [33,65–68]. Such an approach could provide confirmation of the excitation of surface modes as well as shed new light on the role of inhomogeneities in the coherent emission process.

ACKNOWLEDGMENTS

We acknowledge support from the Max Planck-New York Center for Non-Equilibrium Quantum Phenomena and from the Deutsche Forschungsgemeinschaft (DFG, German Research Foundation) via the Cluster of Excellence CUI: Advanced Imaging of Matter (EXC 2056, project ID 390715994). E. D. acknowledges support from AFOSR-MURI: Photonic Quantum Matter Award No. FA95501610323, DARPA DRINQS, the ARO grant ‘‘Control of Many-Body States Using Strong Coherent Light-Matter Coupling in Terahertz Cavities.’’ Work at Columbia University was entirely supported by the Center on Precision-Assembled Quantum Materials, funded through the U.S. National Science Foundation (NSF) Materials Research Science and Engineering Centers (Award No. DMR-2011738).

DATA AVAILABILITY

The data that support the findings of this article are openly available [60].

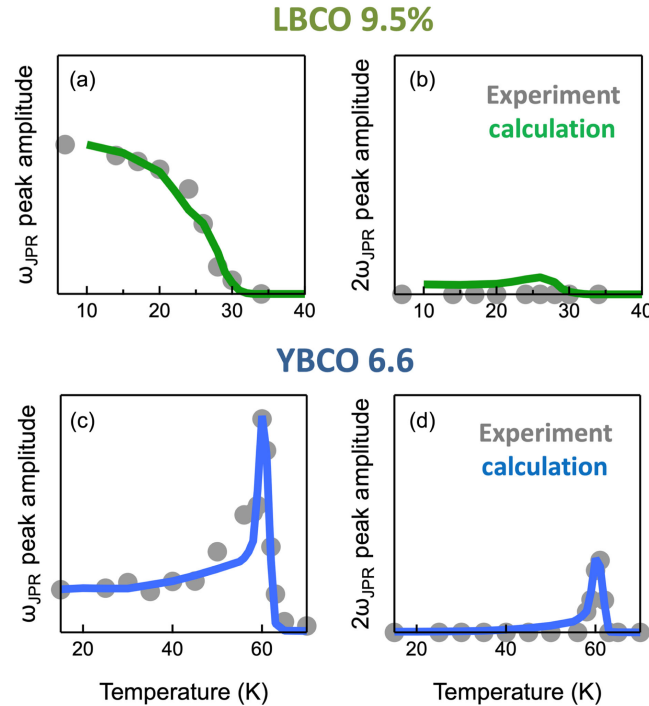


FIG. 5. Comparison between the temperature dependent peak emission amplitude at ω_{JPR} (a),(c) and $2\omega_{\text{JPR}}$ (b),(d) in both LBCO 9.5% and YBCO 6.6, measured experimentally (gray circles) and predicted by the model (full lines). The experimental data in (a)–(b) were taken with a pump fluence of ~ 2.5 mJ/cm², while those in (c)–(d) with ~ 5 mJ/cm².

[1] J. Pettine, P. Padmanabhan, N. Sirica, R. P. Prasankumar, A. J. Taylor, and H.-T. Chen, *Ultrafast terahertz emission*

- from emerging symmetry-broken materials, *Light Sci. Appl.* **12**, 133 (2023).
- [2] S. Yang, L. Cheng, and J. Qi, *Terahertz emission in quantum materials*, *Ultrafast Sci.* **3**, 0047 (2023).
- [3] D. H. Auston, K. P. Cheung, and P. R. Smith, *Picosecond photoconducting Hertzian dipoles*, *Appl. Phys. Lett.* **45**, 284 (1984).
- [4] M. Hangyo, S. Tomozawa, Y. Murakami, M. Tonouchi, M. Tani, Z. Wang, K. Sakai, and S. Nakashima, *Terahertz radiation from superconducting $\text{YBa}_2\text{Cu}_3\text{O}_{7-\delta}$ thin films excited by femtosecond optical pulses*, *Appl. Phys. Lett.* **69**, 2122 (1996).
- [5] T. Kiwa, I. Kawashima, S. Nashima, M. Hangyo, and M. Tonouchi, *Optical response in amorphous GaAs thin films prepared by pulsed laser deposition*, *Jpn. J. Appl. Phys.* **39**, 6304 (2000).
- [6] N. Kida and M. Tonouchi, *Terahertz radiation from magnetoresistive $\text{Pr}_{0.7}\text{Ca}_{0.3}\text{MnO}_3$ thin films*, *Appl. Phys. Lett.* **78**, 4115 (2001).
- [7] D. S. Rana and M. Tonouchi, *Terahertz emission functionality of high-temperature superconductors and similar complex systems*, *Adv. Opt. Mater.* **8**, 1900892 (2020).
- [8] N. Kida, K. Takahashi, and M. Tonouchi, *Effect of charge ordering and disordering on terahertz radiation characteristics of magnetoresistive $\text{Pr}_{0.7}\text{Ca}_{0.3}\text{MnO}_3$ thin films*, *Opt. Lett.* **29**, 2554 (2004).
- [9] K. R. Mavani, D. S. Rana, K. Takahashi, I. Kawayama, H. Murakami, and M. Tonouchi, *Effects of cation disorder on terahertz emission from half-doped manganite thin films*, *Europhys. Lett.* **81**, 17009 (2008).
- [10] K. Takahashi, N. Kida, and M. Tonouchi, *Terahertz radiation by an ultrafast spontaneous polarization modulation of multiferroic BiFeO_3 thin films*, *Phys. Rev. Lett.* **96**, 117402 (2006).
- [11] D. S. Rana, K. Takahashi, K. R. Mavani, I. Kawayama, H. Murakami, and M. Tonouchi, *Structural dependence of terahertz radiation from multiferroic BiFeO_3 thin films*, *Phys. Rev. B* **77**, 024105 (2008).
- [12] D. Talbayev, S. Lee, S. W. Cheong, and A. J. Taylor, *Terahertz wave generation via optical rectification from multiferroic BiFeO_3* , *Appl. Phys. Lett.* **93**, 212906 (2008).
- [13] D. J. Hilton, R. D. Averitt, C. A. Meserole, G. L. Fisher, D. J. Funk, J. D. Thompson, and A. J. Taylor, *Terahertz emission via ultrashort-pulse excitation of magnetic metal films*, *Opt. Lett.* **29**, 1805 (2004).
- [14] E. Beaurepaire, G. M. Turner, S. M. Harrel, M. C. Beard, J.-Y. Bigot, and C. A. Schmuttenmaer, *Coherent terahertz emission from ferromagnetic films excited by femtosecond laser pulses*, *Appl. Phys. Lett.* **84**, 3465 (2004).
- [15] T. Kampfrath, M. Battiato, P. Maldonado, G. Eilers, J. Nötzold, S. Mährlein, V. Zbarsky, F. Freimuth, Y. Mokrousov, S. Blugel, M. Wolf, I. Radu, P. M. Oppeneer, and M. Munzenberg, *Terahertz spin current pulses controlled by magnetic heterostructures*, *Nat. Nanotechnol.* **8**, 256 (2013).
- [16] T. Kampfrath, A. Sell, G. Klatt, A. Pashkin, S. Mährlein, T. Dekorsy, M. Wolf, M. Fiebig, A. Leitenstorfer, and R. Huber, *Coherent terahertz control of antiferromagnetic spin waves*, *Nat. Photonics* **5**, 31 (2011).
- [17] R. V. Mikhaylovskiy, E. Hendry, V. V. Kruglyak, R. V. Pisarev, Th. Rasing, and A. V. Kimel, *Terahertz emission spectroscopy of laser-induced spin dynamics in TmFeO_3 and ErFeO_3 orthoferrites*, *Phys. Rev. B* **90**, 184405 (2014).
- [18] R. V. Mikhaylovskiy, T. J. Huisman, A. I. Popov, A. K. Zvezdin, Th. Rasing, R. V. Pisarev, and A. V. Kimel, *Terahertz magnetization dynamics induced by femtosecond resonant pumping of Dy^{3+} subsystem in the multisublattice antiferromagnet DyFeO_3* , *Phys. Rev. B* **92**, 094437 (2015).
- [19] R. V. Mikhaylovskiy, T. J. Huisman, V. A. Gavrichkov, S. I. Polukeev, S. G. Ovchinnikov, D. Afanasiev, R. V. Pisarev, Th. Rasing, and A. V. Kimel, *Resonant pumping of d-d crystal field electronic transitions as a mechanism of ultrafast optical control of the exchange interactions in iron oxides*, *Phys. Rev. Lett.* **125**, 157201 (2020).
- [20] M. Tonouchi, M. Tani, Z. Wang, S. Sakai, S. Tomozawa, M. Hangyo, Y. Murakami, and S. Nakashima, *Ultrashort electromagnetic pulse radiation from YBCO thin films excited by femtosecond optical pulse*, *Jpn. J. Appl. Phys.* **35**, 2624 (1996).
- [21] M. Tonouchi, A. Fujimaki, K. Tanabe, K. Enpuku, K. Nikawa, and T. Kobayashi, *Recent topics in high-Tc superconductive electronics*, *Jpn. J. Appl. Phys.* **44**, 7735 (2005).
- [22] Y. Tominari, T. Kiwa, H. Murakami, M. Tonouchi, H. Wald, P. Seidel, and H. Schneidewind, *Resonant terahertz radiation from $\text{Tl}_2\text{Ba}_2\text{CaCu}_2\text{O}_{8+\delta}$ thin films by ultrafast optical pulse excitation*, *Appl. Phys. Lett.* **80**, 3147 (2002).
- [23] L. Ozyuzer, A. E. Koshelev, C. Kurter, N. Gopalsami, Q. Li, M. Tachiki, K. Kadowaki, T. Yamamoto, H. Minami, H. Yamaguchi, T. Tachiki, K. E. Gray, W.-K. Kwok, and U. Welp, *Emission of coherent THz radiation from superconductors*, *Science* **318**, 1291 (2007).
- [24] U. Welp, K. Kadowaki, and R. Kleiner, *Superconducting emitters of THz radiation*, *Nat. Photonics* **7**, 702 (2013).
- [25] E. A. Borodianskyi and V. M. Krasnov, *Josephson emission with frequency span 1–11 THz from small $\text{Bi}_2\text{Sr}_2\text{CaCu}_2\text{O}_{8+\delta}$ mesa structures*, *Nat. Commun.* **8**, 1742 (2017).
- [26] D. Nicoletti, M. Buzzi, M. Fechner, P. E. Dolgirev, M. H. Michael, J. B. Curtis, E. Demler, G. D. Gu, and A. Cavalleri, *Coherent emission from surface Josephson plasmons in striped cuprates*, *Proc. Natl. Acad. Sci. U.S.A.* **119**, e2211670119 (2022).
- [27] M. Hücker, M. v. Zimmermann, G. D. Gu, Z. J. Xu, J. S. Wen, Guangyong Xu, H. J. Kang, A. Zheludev, and J. M. Tranquada, *Stripe order in superconducting $\text{La}_{2-x}\text{Ba}_x\text{CuO}_4$ ($0.095 \leq x \leq 0.155$)*, *Phys. Rev. B* **83**, 104506 (2011).
- [28] J. M. Tranquada, B. J. Sternlieb, J. D. Axe, Y. Nakamura, and S. Uchida, *Evidence for stripe correlations of spins and holes in copper oxide superconductors*, *Nature (London)* **375**, 561 (1995).
- [29] E. Berg, E. Fradkin, E.-A. Kim, S. A. Kivelson, V. Oganesyan, J. M. Tranquada, and S. C. Zhang, *Dynamical layer decoupling in a stripe-ordered high- T_c superconductor*, *Phys. Rev. Lett.* **99**, 127003 (2007).
- [30] E. Berg, E. Fradkin, S. A. Kivelson, and J. M. Tranquada, *Striped superconductors: How spin, charge and superconducting orders intertwine in the cuprates*, *New J. Phys.* **11**, 115004 (2009).

- [31] P. E. Dolgirev, M. H. Michael, J. B. Curtis, D. Nicoletti, M. Buzzi, M. Fechner, A. Cavalleri, and E. Demler, *Theory for anomalous terahertz emission in striped cuprate superconductors*, *Phys. Rev. B* **108**, L180508 (2023).
- [32] P. E. Dolgirev, M. H. Michael, J. B. Curtis, D. E. Parker, D. Nicoletti, M. Buzzi, M. Fechner, A. Cavalleri, and E. Demler, *Optically induced umklapp shift currents in striped cuprates*, *Phys. Rev. B* **109**, 045150 (2024).
- [33] H. T. Stinson, J. S. Wu, B. Y. Jiang, Z. Fei, A. S. Rodin, B. C. Chapler, A. S. McLeod, A. Castro Neto, Y. S. Lee, M. M. Fogler, and D. N. Basov, *Infrared nanospectroscopy and imaging of collective superfluid excitations in anisotropic superconductors*, *Phys. Rev. B* **90**, 014502 (2014).
- [34] S. Savel'ev, V. Yampolskii, and F. Nori, *Surface Josephson plasma waves in layered superconductors*, *Phys. Rev. Lett.* **95**, 187002 (2005).
- [35] S. Savel'ev, V. Yampol'skii, A. Rakhmanov, and F. Nori, *Terahertz Josephson plasma waves in layered superconductors: Spectrum, generation, nonlinear and quantum phenomena*, *Rep. Prog. Phys.* **73**, 026501 (2010).
- [36] G. Ghiringhelli *et al.*, *Long-range incommensurate charge fluctuations in (Y, Nd)Ba₂Cu₃O_{6+x}*, *Science* **337**, 821 (2012).
- [37] T. Wu, H. Mayaffre, S. Krämer, M. Horvatić, C. Berthier, W. N. Hardy, R. Liang, D. A. Bonn, and M.-H. Julien, *Magnetic-field-induced charge-stripe order in the high-temperature superconductor YBa₂Cu₃O_y*, *Nature (London)* **477**, 191 (2011).
- [38] J. Chang, E. Blackburn, A. T. Holmes, N. B. Christensen, J. Larsen, J. Mesot, R. Liang, D. A. Bonn, W. N. Hardy, A. Watenphul, M. v. Zimmermann, E. M. Forgan, and S. M. Hayden, *Direct observation of competition between superconductivity and charge density wave order in YBa₂Cu₃O_{6.67}*, *Nat. Phys.* **8**, 871 (2012).
- [39] S. Blanco-Canosa, A. Frano, E. Schierle, J. Porras, T. Loew, M. Minola, M. Bluschke, E. Weschke, B. Keimer, and M. Le Tacon, *Resonant x-ray scattering study of charge-density wave correlations YBa₂Cu₃O_{6+x}*, *Phys. Rev. B* **90**, 054513 (2014).
- [40] M. Hücker, N. B. Christensen, A. T. Holmes, E. Blackburn, E. M. Forgan, Ruixing Liang, D. A. Bonn, W. N. Hardy, O. Gutowski, M. v. Zimmermann, S. M. Hayden, and J. Chang, *Competing charge, spin, and superconducting orders in underdoped YBa₂Cu₃O_y*, *Phys. Rev. B* **90**, 054514 (2014).
- [41] See Supplemental Material at <http://link.aps.org/supplemental/10.1103/lbph-97sg> for additional data sets, fitting model for THz emission in time domain, equilibrium Josephson plasma frequency of YBa₂Cu₃O_{6.6}, analysis of the emission bandwidth, amplitude scaling of the emission peaks, model for coherent THz emission activated by superconducting fluctuations, which includes Refs. [26,27,31,32,39,42–59].
- [42] R. Boyd, *Nonlinear Optics*, 3rd ed. (Academic Press, Waltham, 2008).
- [43] N. Taherian, M. Först, A. Liu, M. Fechner, D. Pavicevic, A. von Hoegen, E. Rowe, Y. Liu, S. Nakata, B. Keimer, E. Demler, M. H. Michael, and A. Cavalleri, *Probing amplified Josephson plasmons in YBa₂Cu₃O_{6+x} by multidimensional spectroscopy*, *npj Quantum Mater.* **10**, 54 (2025).
- [44] A. Gómez Salvador, P. E. Dolgirev, M. H. Michael, A. Liu, D. Pavixćević, M. Fechner, A. Cavalleri, and E. Demler, *Principles of two-dimensional terahertz spectroscopy of collective excitations: The case of Josephson plasmons in layered superconductors*, *Phys. Rev. B* **110**, 094514 (2024).
- [45] D. van der Marel and A. Tsetkov, *Transverse optical plasmons in layered superconductors*, *Czech. J. Phys.* **46**, 3165 (1996).
- [46] D. van der Marel and A. A. Tsvetkov, *Transverse-optical Josephson plasmons: Equations of motion*, *Phys. Rev. B* **64**, 024530 (2001).
- [47] D. Munzar, C. Bernhard, A. Golnik, J. Humlíček, and M. Cardona, *Anomalies of the infrared-active phonons in underdoped YBa₂Cu₃O_y as evidence for the intra-bilayer Josephson effect*, *Solid State Commun.* **112**, 365 (1999).
- [48] N. Sellati, F. Gabriele, C. Castellani, and L. Benfatto, *Generalized Josephson plasmons in bilayer superconductors*, *Phys. Rev. B* **108**, 014503 (2023).
- [49] J. Fiore, N. Sellati, F. Gabriele, C. Castellani, G. Seibold, M. Udina, and L. Benfatto, *Investigating Josephson plasmons in layered cuprates via nonlinear terahertz spectroscopy*, *Phys. Rev. B* **110**, L060504 (2024).
- [50] A. von Hoegen, M. Fechner, M. Först, N. Taherian, E. Rowe, A. Ribak, J. Porras, B. Keimer, M. Michael, E. Demler, and A. Cavalleri, *Amplification of superconducting fluctuations in driven YBa₂Cu₃O_{6+x}*, *Phys. Rev. X* **12**, 031008 (2022).
- [51] M. H. Michael, A. von Hoegen, M. Fechner, M. Först, A. Cavalleri, and E. Demler, *Parametric resonance of Josephson plasma waves: A theory for optically amplified interlayer superconductivity in YBa₂Cu₃O_{6+x}*, *Phys. Rev. B* **102**, 174505 (2020).
- [52] G. Homann, M. H. Michael, J. G. Cosme, and L. Mathey, *Dissipationless counterflow currents above T_c in bilayer superconductors*, *Phys. Rev. Lett.* **132**, 096002 (2024).
- [53] M. H. Michael, D. De Santis, E. Demler, and P. A. Lee, *Giant dynamical paramagnetism in the driven pseudogap phase of YBa₂Cu₃O_{6+x}*, [arXiv:2410.12919](https://arxiv.org/abs/2410.12919).
- [54] D. Nicoletti, D. Fu, O. Mehio, S. Moore, A. S. Disa, G. D. Gu, and A. Cavalleri, *Magnetic-field tuning of light-induced superconductivity in striped La_{2-x}Ba_xCuO₄*, *Phys. Rev. Lett.* **121**, 267003 (2018).
- [55] S. Kaiser, C. R. Hunt, D. Nicoletti, W. Hu, I. Gierz, H. Y. Liu, M. Le Tacon, T. Loew, D. Haug, B. Keimer, and A. Cavalleri, *Optically induced coherent transport far above T_c in underdoped YBa₂Cu₃O_{6+δ}*, *Phys. Rev. B* **89**, 184516 (2014).
- [56] C. R. Hunt, D. Nicoletti, S. Kaiser, D. Pröpper, T. Loew, J. Porras, B. Keimer, and A. Cavalleri, *Dynamical decoherence of the light induced interlayer coupling in YBa₂Cu₃O_{6+δ}*, *Phys. Rev. B* **94**, 224303 (2016).
- [57] K. Katsumi, N. Tsuji, Y. I. Hamada, R. Matsunaga, J. Schneeloch, R. D. Zhong, G. D. Gu, H. Aoki, Y. Gallais, and R. Shimano, *Higgs mode in the d-wave superconductor Bi₂Sr₂CaCu₂O_{8+x} driven by an intense terahertz pulse*, *Phys. Rev. Lett.* **120**, 117001 (2018).
- [58] H. Chu *et al.*, *Phase-resolved Higgs response in superconducting cuprates*, *Nat. Commun.* **11**, 1793 (2020).
- [59] J. Yuan *et al.*, *Dynamical interplay between superconductivity and pseudogap in cuprates as revealed by terahertz third-harmonic generation spectroscopy*, *Sci. Adv.* **10**, eadg9211 (2024).

- [60] Source data for Figs. 1,2,3,4, and 5 can be found at Nicoletti, Daniele. 2025. "Enhanced Coherent Terahertz Emission from Critical Superconducting Fluctuations in $\text{YBa}_2\text{Cu}_3\text{O}_{6.6}$ ". Edmond. [10.17617/3.NFMM6C](https://doi.org/10.17617/3.NFMM6C).
- [61] T. Dekorsy, H. Auer, H. J. Bakker, H. G. Roskos, and H. Kurz, *THz electromagnetic emission by coherent infrared-active phonons*, *Phys. Rev. B* **53**, 4005 (1996).
- [62] A. Liu, D. Pavićević, M. H. Michael, A. Gómez Salvador, P. E. Dolgirev, M. Fechner, A. S. Disa, P. M. Lozano, Q. Li, G. D. Gu, E. Demler, and A. Cavalleri, *Probing inhomogeneous cuprate superconductivity by terahertz Josephson echo spectroscopy*, *Nat. Phys.* **20**, 1751 (2024).
- [63] P. E. Dolgirev, A. Zong, M. H. Michael, J. B. Curtis, D. Podolsky, A. Cavalleri, and E. Demler, *Periodic dynamics in superconductors induced by an impulsive optical quench*, *Commun. Phys.* **5**, 234 (2022).
- [64] R. Merlin, *Generating coherent THz phonons with light pulses*, *Solid State Commun.* **102**, 207 (1997).
- [65] H. T. Stinson, A. Sternbach, O. Najera, R. Jing, A. S. Mcleod, T. V. Slusar, A. Mueller, L. Anderegg, H. T. Kim, M. Rozenberg, and D. N. Basov, *Imaging the nanoscale phase separation in vanadium dioxide thin films at terahertz frequencies*, *Nat. Commun.* **9**, 3604 (2018).
- [66] R. Jing, Y. Shao, Z. Fei, C. F. Bowen Lo, R. A. Vitalone, F. L. Ruta, J. Staunton, W. J.-C. Zheng, A. S. Mcleod, Z. Sun, B.-Y. Jiang, X. Chen, M. M. Fogler, A. J. Millis, M. Liu, D. H. Cobden, X. Xu, and D. N. Basov, *Terahertz response of monolayer and few-layer WTe_2 at the nanoscale*, *Nat. Commun.* **12**, 5594 (2021).
- [67] R. A. Vitalone, B. S. Jessen, R. Jing, D. J. Rizzo, S. Xu, V. Hsieh, M. Cothrine, D. G. Mandrus, L. Wehmeier, G. L. Carr, V. Bisogni, C. R. Dean, J. C. Hone, M. Liu, M. I. Weinstein, M. M. Fogler, and D. N. Basov, *Charge transfer plasmonics in bespoke graphene/ α - RuCl_3 cavities*, *ACS Nano* **18**, 29648 (2024).
- [68] S. Xu, Y. Li, R. A. Vitalone, R. Jing, A. J. Sternbach, S. Zhang, J. Ingham, M. Delor, J. W. McIver, M. Yankowitz, R. Queiroz, A. J. Millis, M. M. Fogler, C. R. Dean, A. N. Pasupathy, J. Hone, M. Liu, and D. N. Basov, *Electronic interactions in Dirac fluids visualized by nano-terahertz spacetime interference of electron-photon quasiparticles*, *Sci. Adv.* **10**, eado5553 (2024).